Supplemental Material

Huttner, HB, et al.

Meningioma growth dynamics assessed by radiocarbon retrospective birth dating

Content

Supplementary methods.

The age-structured Gompertz model

The mathematical model consists of a linear partial differential equation with an age-structure:

$$\frac{\partial n(x,t)}{\partial t} + \frac{\partial n(x,t)}{\partial x} = 0,$$
$$n(x,0) = N_0 \delta(x),$$
$$n(0,t) = \alpha N(t) \ln\left(\frac{K}{N(t)}\right).$$

Here, $n(x,t)$ is the density of cells of age x at time t, N_0 is the initial number of cells and the Dirac delta function $\delta(x)$ ensures that all cells initially have an age $x = 0$. The boundary condition $n(0,t)$ describes the addition of new cells in time following a Gompertz type of growth. $N(t)$ is the total number of cells and can be calculated by summing all cells of all ages, $N(t) = \int_0^t n(x,t)dx$. The average age of cells can be calculated using the following formula: $\langle a \rangle = \frac{\int_0^t x n(x,t)dx}{N(t)}$.

The solution of the age-structured Gompertz equation can be given explicitly by:

$$n(x,t) = \begin{cases} N_0 \delta(x-t) + \alpha K \ln\left(\frac{K}{N_0}\right) e^{-\alpha(t-x)} \, e^{\ln\left(\frac{N_0}{K}\right) e^{-\alpha(t-x)}}, t \geq x \\ 0, x > t \end{cases}$$

In this model, we made several assumptions regarding the cell dynamics during aging. First, we assumed that there is no cell death (0 on the right hand side of the first equation of the model). Second, we assumed that a cell is born at age zero (boundary condition at $x = 0$). Third, we assumed that mother cells retain their age when they divide.

Patients 1-5:

To estimate the age of the tumor, we relied on two main experimental data for each patient: the average age of cells and the tumor size measured at two different time points of its evolution (table 1). The method consists of finding the appropriate values of the coefficients (t,α,K) such that the quantities calculated using the model fit with their corresponding experimental data. For that, we defined the following cost function:

$$J_1 = \left|\tilde{V}_1 - V_{d1}\right|^2 + \left|\tilde{V}_2 - V_{d2}\right|^2 + \left|\langle\tilde{a}\rangle - \langle a_d\rangle\right|^2,$$

where the model predicted values $\tilde{V}_1$, $\tilde{V}_2$ and $\langle\tilde{a}\rangle$ are the tumor volume at the time of the first MRI scan, the tumor volume at the time of the second MRI scan, and the average age, respectively. V_{d1}, V_{d2} and a_d are the corresponding experimental data. To find the age of the tumor, the problem reduces to a minimization problem. Find:

$$\min_{(t,\alpha,K)} J_1(t,\alpha,K;\tilde{V}_1,\tilde{V}_2,\langle\tilde{a}\rangle),$$

such that (t,α,K) belong to an admissible set of values. This means that the time of growth t should not exceed the patient age. The time interval between the two MRI scans (times at which V_{d1} and V_{d2} are collected) should also be respected. The coefficients α and K should be chosen so that the value of the growth rate $\alpha\ln\left(\frac{K}{N}\right)$ does not exceed the growth rate induced by the Ki-67 index. This is due to the fact that we do only consider net growth. This may not reflect the heterogeneity of the population, because there might be another subset of non-proliferating cells. Therefore, the Ki-67 index, gave us an upper bound for the growth rate. Due to the fact that we had three parameters to estimate and three experimental data points to fit, the solution to the minimization problem was unique. We found a unique tumor age, a proliferation coefficient and a carrying capacity that fit the experimental data. We calculated also the lag time for each growth curve. The lag time is defined to be the period after which a noticeable growth starts to be seen. It can be calculated by taking the intersection of the tangent line at the inflexion point of the growth curve and the horizontal line $y = N_0$ [1]. Results are given in table 2.

Patients 6-14:

For each patient the average age of cells and only one measurement for the tumor volume, which was calculated during the tumor extraction surgery (table 3), was available. Having two data points and three parameters to estimate for each patient led to non uniqueness problems in the estimation procedure. To circumvent this difficulty, we looked for additional data about meningioma growth rate in the literature. We used results taken from the work of Nakamura and colleagues. In this study authors investigated the relation between the patient age and the growth rate of meningioma [2].

Following the approach used for the first set of patients, we estimated the age of the tumor relying on three main experimental data for each patient: the average age of cells, the tumor size and the absolute growth rate calculated from Nakamura data. The new cost function reads:

$$J_2 = \left|\tilde{V} - V_d\right|^2 + \left|\langle \tilde{a} \rangle - \langle a_d \rangle\right|^2 + \left|\tilde{\gamma} - \gamma_d\right|^2,$$

where the model predicted values $\tilde{V}, \langle \tilde{a} \rangle$ and $\tilde{\gamma}$ are the volume, the average age of cells and the absolute growth rate, respectively. V_d, a_d and γ_d are the corresponding experimental data. Similarly, by minimizing the cost function J_2, we were able to estimate the tumor age for each patient. Results are given in table 4.

Tables:

Table 1: Experimental data for the first 5 patients.

Patient	Birthday	Date of operation	Ki-67 index	Tumor size at surgery	Tumor size beforehand	Months between MRI scans	Average age of cells

1	Apr. 1938	Oct. 2013	2,41	62,22	5,32	85	4.20
2	Oct. 1935	May. 2014	1,79	96,59	56,16	33	4.10
3	Sep. 1955	Feb. 2009	1,49	145	103	60	5.70
4	Apr. 1952	Jul. 2003	0,61	2,51	2,26	52	9.40
5	Apr. 1964	Sep. 2014	12,02	9,36	1,54	11	0.70

Table 2: Modeling results for the first 5 patients.

Patient	Carrying capacity K	Proliferation coefficient □	Estimated tumor age	Lag time
1	72.7689	0.3975	12.7632	5.5831
2	609.1652	0.0939	28.664	24.5031
3	146.2822	0.7370	10.8267	3.0486
4	2.6127	0.2966	21.2139	7.0012
5	9.5251	5.0683	1.4168	0.4211

Table 3: Experimental data for the patients 6-14.

Patient	Birthday	Date of operation	Average age of cells (y)	Ki-67 index	Tumor size (cm3)
6	Aug. 1932	Apr. 2004	3.0	1.0	50.5
7	May. 1933	Jan. 2001	3.3	0.9	1.7
8	Dec. 1939	Nov. 2001	3.8	0.7	44.5
9	Dec. 1948	Dec. 1996	3.7	1.1	7.5
10	July. 1953	Jan. 2003	2.2	1.2	6.25
11	Sep. 1963	Jan. 2002	2.4	0.6	2.25
12	Oct. 1966	June. 2011	6.4	0.8	38.5
13	Jan. 1969	Feb. 2011	4.9	1.0	21
14	June. 1967	Mar. 2011	0.1	7.1	168

Table 4: Modeling results for the second set of patients.

Patient	Proliferation coefficient ρ	Carrying capacity K	Tumor age	Lag time
6	0.1598	271.0654	18.5091	14.2583
7	0.0748	59.1068	27.2624	29.6740
8	0.1438	187.1468	21.7585	15.7387
9	0.0943	76.6468	26.3990	23.5863
10	0.1274	126.0214	17.4661	17.6163
11	0.0995	82.4942	20.2259	22.3877
12	0.1132	86.6916	31.1183	19.6672
13	0.1056	91.3638	28.6257	21.1330
14	0.6486	4.1422e+08	1.5887	4.1725

Bibliography

[1] I. a. M. Swinnen, K. Bernaerts, E. J. J. Dens, A. H. Geeraerd, et J. F. Van Impe, « Predictive modelling of the microbial lag phase: a review », *Int. J. Food Microbiol.*, vol. 94, n° 2, p. 137-159, juill. 2004.

[2] M. Nakamura, F. Roser, J. Michel, C. Jacobs, et M. Samii, « The natural history of incidental meningiomas », *Neurosurgery*, vol. 53, n° 1, p. 62-70-71, juill. 2003.

Supplementary Table 1. Patient demographics, clinical and radiological characteristics as well as neuropathological findings of all patients with meningiomas.

	PARAMETERS		CLINICAL		RADIOLOGICAL			TREATMENT	HISTOLOGICAL			
PATIENTS	Age	Sex	De-novo diagnosis	Symptomatic	Tumor Size pre-OP (cc)	Tumor size previous MRI (months before surgery)	Location	Date of surgery	WHO grade	type	Ki-67 index	cells (1/mm3)
Patient 1	75	female	0	0	62.2	5.3 (85 months)	Sphenoidal left	10/2013	1	meningothelial	2.4%	7632
Patient 2	79	female	0	0	96.6	56.1 (33 months)	Falx parietal left	05/2014	1	fibrous	1.7%	6264
Patient 3	54	male	0	0	144.0	103 (60 months)	Parasagittal parietal right	02/2009	1	meningothelial	1.4%	5904
Patient 4	51	male	0	0	2.6	2.2 (52 months)	Suprasellar right	07/2003	1	fibrous	0.6%	5712
Patient 5	50	female	0	0	9.4	1.5 (11 months)	Sphenoidal right	09/2014	**2**	atypical	12.2%	3728
Patient 6	72	female	1	1	50.5	n.a.	Convexity occipital left	10/2004	1	meningothelial	1.0%	4409
Patient 7	68	female	1	1	2.7	n.a.	Clinoid left	01/2001	1	meningothelial	0.9%	5177
Patient 8	62	female	1	1	44.5	n.a.	Falx frontal right	03/2001	1	fibrous	0.7%	5692
Patient 9	48	female	1	1	7.5	n.a.	Temporal left	12/1996	1	fibrous	1.1%	6101
Patient 10	50	female	1	1	6.3	n.a.	Convexity parietal left	09/2003	1	meningothelial	1.2%	5594
Patient 11	39	female	1	1	2.6	n.a.	frontobasal	09/2002	1	meningothelial	0.6%	5841
Patient 12	45	female	1	1	38.5	n.a.	Convexity frontal right	02/2011	1	fibrous	0.8%	6015
Patient 13	42	female	1	1	21.0	n.a.	Cerebellar left	04/2011	1	fibrous	1.0%	6223
Patient 14	44	male	1	1	168.0	n.a.	Parasagittal frontal left	07/2011	**2**	atypical	7.1%	4912

Supplementary Figure 1: ^{14}C concentrations of meningioma in comparison to no-turnover control samples.

Genomic ^{14}C concentrations of cortical and cerebellar neurons are not different from atmospheric ^{14}C values at birth (plotted at the time of birth, black triangle), demonstrating no postnatal cellular turnover of these populations (Bergmann et al., 2012; Huttner et al., 2014). Genomic ^{14}C concentrations from WHO grade I (blue dots) and WHO grade II (red dots) meningioma show substantial deviation from the atmospheric ^{14}C curve indicating the generation of new cells during the course of life (tumor growth). All data points are plotted at the birth of the patient. The black curve indicates atmospheric ^{14}C concentrations measured over the last decades in the northern hemisphere.

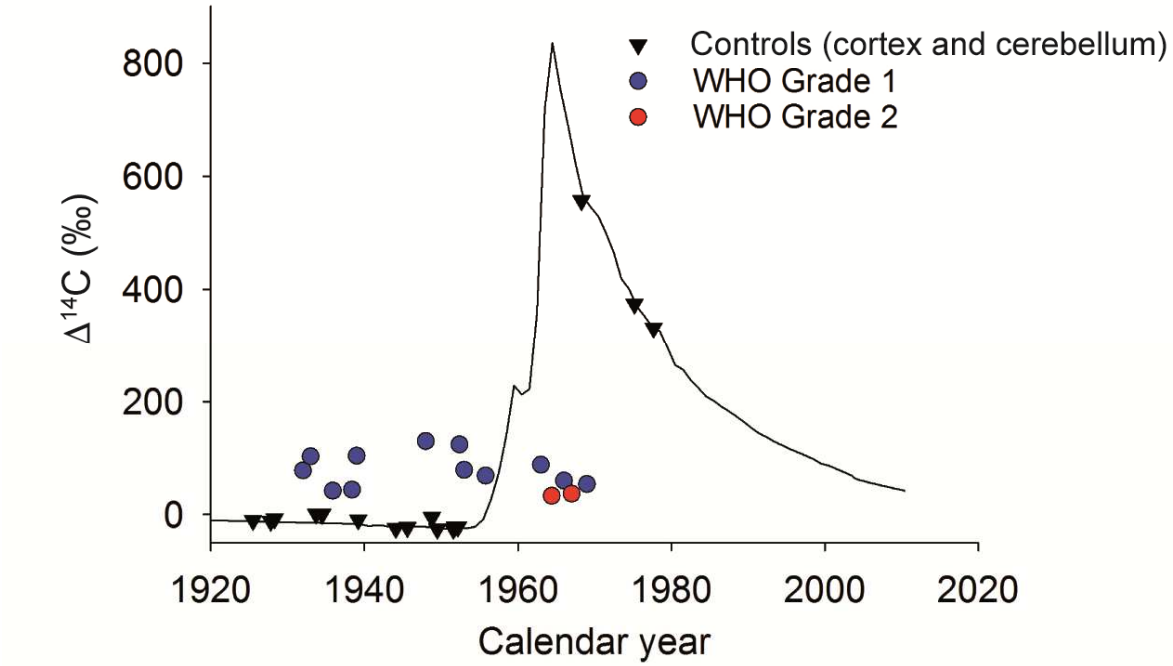

Supplementary Figure 2: Growth curves of meningiomas

Model-fitted meningioma growth curves given for patient 6 to 13 with benign fibrous (dark blue), meningothelial (light blue), and atypical (red) meningiomas. The growth curves were estimated using nonlinear least-square with uniform weighting. Parameters were based on ^{14}C measurements, histological data and on volumetric measurement of one MRI obtained prior to surgery (see Methods).

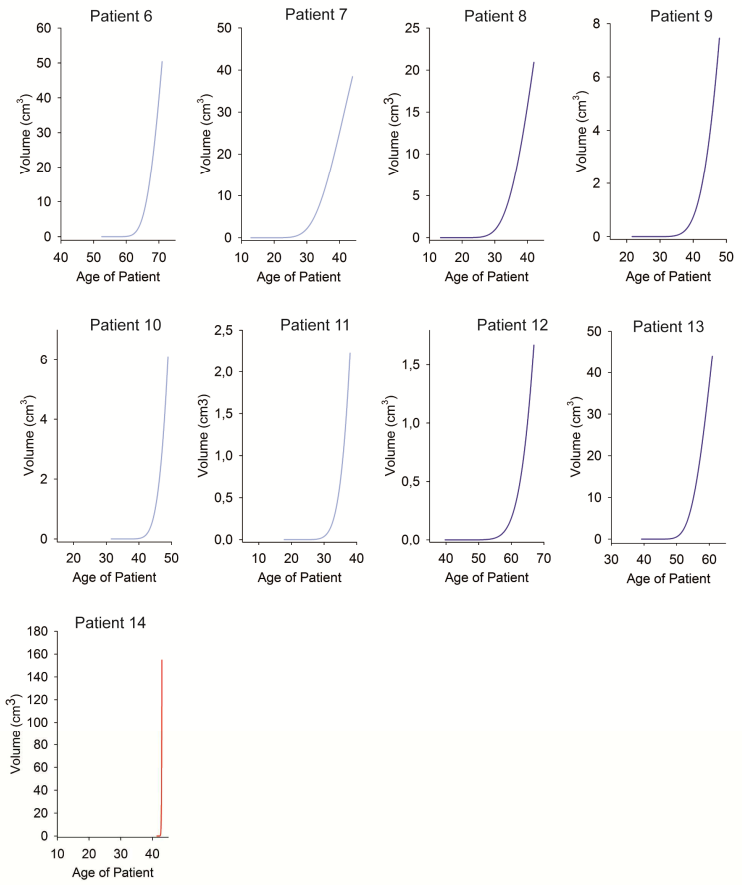

Supplementary Figure 3: Correlations with age of meningiomas.

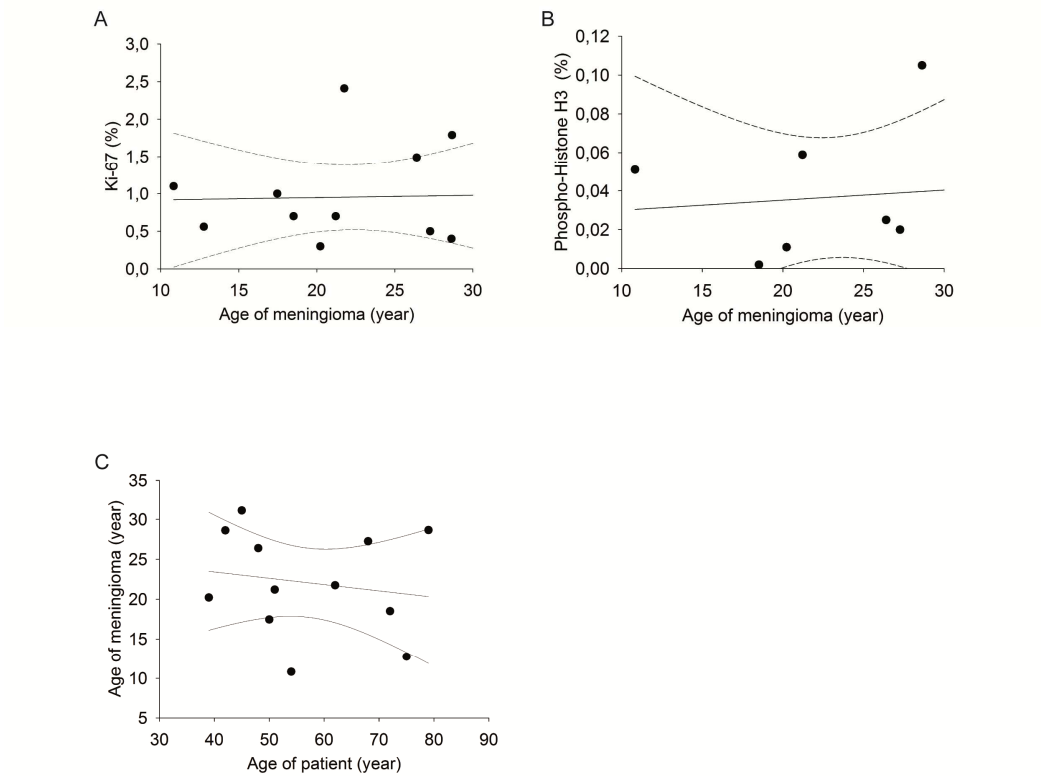

No significant correlations of age of meningiomas with (A) Ki-67 labeling index, phospho-Histone H3 (B) or with (C) age of patient.